

Effects of Nitro-L-Arginine on Blood Pressure and Cardiac Index in Anesthetized Rats: A Pharmacokinetic-Pharmacodynamic Analysis

Mohammad A. Tabrizi-Fard¹ and Ho-Leung Fung^{1,2}

Received January 14, 1998; accepted April 1, 1998

Purpose. Nitric oxide synthase (NOS) inhibitors such as Nitro-L-arginine (L-NA) are being considered for the management of hypotension observed in septic shock. However, little information is available regarding the pharmacokinetic and pharmacodynamic properties of these agents. Our objective was to examine the relationships between L-NA plasma concentration and various hemodynamic effects such as cardiac index (CI), mean arterial pressure (MAP), and heart rate (HR) elicited by L-NA administration in rats.

Methods. L-NA was infused at doses between 2.5–20 mg/kg/hr in anesthetized rats over one hour. Hemodynamic effects and plasma L-NA levels were determined.

Results. Infusion of L-NA resulted in dose-dependent increases in MAP and systemic vascular resistance (SVR), decreases in CI, and minimal change in HR. The relationships between the hemodynamic effects and plasma L-NA levels were not monotonic, and hysteresis was observed. Using nonparametric analysis, the equilibration half-time ($t_{1/2,keo}$) between plasma L-NA and the hypothetical effect site was determined to be 51.5 ± 6.6 min, 42.4 ± 10.1 min, 43.4 ± 9.0 min for MAP, CI, and SVR, respectively ($n = 14$). The E_{max} and EC_{50} values obtained were $+32.5 \pm 8.4$ and 2.6 ± 1.3 $\mu\text{g/ml}$ for MAP and -52.9 ± 15.6 and 3.7 ± 1.8 $\mu\text{g/ml}$ for CI, respectively.

Conclusions. Although L-NA can bring about beneficial elevation of MAP, such effect is always accompanied by a stronger effect on CI depression. Dose escalation of L-NA may bring about detrimental negative inotropic effect and loss of therapeutic efficacy.

KEY WORDS: nitric oxide synthase (NOS); nitric oxide (NO); nitro-L-arginine (L-NA); pharmacokinetics (PK); pharmacodynamics (PD); hemodynamic effects.

INTRODUCTION

Nitric oxide (NO) is a potent endogenous vasodilator that regulates vascular tone and organ perfusion both in health and disease (1). NO is formed endogenously from the oxidation of the terminal guanidino nitrogen of the amino acid L-arginine by the enzyme nitric oxide synthase (NOS), several isoforms of which have now been identified (1). Two constitutive isoforms, neuronal (NOS I) and endothelial (NOS III), are expressed in various tissues and generate small amounts of NO. Inflammatory stimuli such as cytokines and bacterial lipopolysaccharide (LPS) induce the expression of another isoform (NOS II). The

large quantity of NO produced in this manner contributes to the profound hypotension observed in septic shock (1). Thus, inhibition of this isoform may be useful in the therapeutic management of this disease (2,3).

L-arginine analogs such as nitro-L-arginine (L-NA) and monomethyl-L-arginine (L-NMMA) have been identified as NOS inhibitors. Administration of these compounds to animals and humans, with or without septic shock, brings about beneficial elevation in mean arterial pressure (MAP), but also significant depression of cardiac output (CO), thus reducing the therapeutic effectiveness of these agents (2,4,5). In several studies, large doses of NOS inhibitor have actually been shown to worsen the outcome of septic shock (5–7).

The pharmacokinetic/pharmacodynamic relationships of NOS inhibitors have not been reported. It is therefore not known whether the beneficial effect (MAP elevation) can be separated from the side-effect (CO depression) by judicious selection of an appropriate range of plasma inhibitor concentrations. In the present study, we administered the prototype NOS inhibitor, L-NA, in several doses to produce a range of plasma concentrations, and examined how these concentrations were related to the hemodynamic effects of MAP, CO and heart rate (HR). The animal preparation used was the anesthetized rat.

METHODS

Materials

L-NA, theophylline (anhydrous crystals), heptane sulphonic acid (sodium salt), were purchased from Sigma chemical company (St. Louis, MO, U.S.A.). Thiobutabarbital sodium (Inactin[®]) was obtained from RBI (Natick, MA, U.S.A.). All solvents used were of HPLC grade (Fisher Scientific, Pittsburgh, PA, U.S.A.).

HPLC Assay

Plasma concentrations of L-NA were analyzed by a reversed-phase HPLC method reported previously (8). In brief, plasma proteins were precipitated with 70–72% perchloric acid after addition of the internal standard (theophylline, 1 mM). The resultant supernatant was neutralized with NaOH (50% W/V) and a 50- μl aliquot of the resultant sample was injected into a C-8 reversed-phase Ultrasphere[®] column (250 \times 4.6 (i.d.) mm, 5 μm) which was preceded by a 45 \times 4.6 (i.d.) mm guard column (both from Beckman, San Ramon, CA, U.S.A.). The mobile phase used was 18.5 mM heptane sulphonic acid/10% methanol (pH = 2.7) at 1.5 ml/min and UV detection was accomplished at 280 nm. The sensitivity limit of the assay in plasma samples was 0.5 $\mu\text{g/ml}$.

Animal Studies

Two to three days before the hemodynamic experiment, male Sprague-Dawley rats (372 \pm 47 g) were anesthetized with ketamine-xylazine (90–10 mg/kg) for cannula implantation. The tip of one cannula (Silastic, 0.025 in. i.d., 0.045 in. o.d.) was placed in the right atrium via the right jugular vein for administration of room-temperature saline (100 μl) and construction of thermodilution curves for calculation of CO (Columbus

¹ Department of Pharmaceutics, School of Pharmacy, State University of New York at Buffalo, Buffalo, New York 14260.

² To whom correspondence should be addressed. (e-mail: HLFung@acsu.buffalo.edu)

instruments, Cardiomax-II®, Columbus, Ohio). The left femoral artery (using polyethylene tubing, 0.011 in. i.d., 0.024 in. i.d.) and vein (using polyethylene tubing, 0.023 in. i.d., 0.038 in. o.d.) were cannulated for the measurements of MAP and infusion of the drug or saline, respectively. On the day of the study, animals were anesthetized with i.p. injection of thiobutabarbital sodium (120 mg/kg). The trachea was cannulated to allow spontaneous respiration. The right carotid artery was cannulated with a thermocouple microprobe (Type IT-21, Physitemp, Clifton, NJ), the tip of which was placed in the aortic arch just distal to the aortic valve. The proper distances for insertion of the jugular vein cannula (4 cm from the point of insertion) and carotid artery microprobe (3 cm from the point of insertion) were determined in preliminary experiments using animals of the same sex and weight. At the end of each study, the cannulas were checked visually to assure proper placement. Blood temperature was monitored with the aortic microprobe and maintained with a heated pad between 36°C to 37°C throughout the study. The left femoral artery catheter was connected to the Cardiomax-II® via a Gould transducer (Gould Statham Instruments Inc., Hato Rey, Puerto Rico) for electronic measurements of MAP and heart rate. The right femoral artery was cannulated for blood sampling. Periodically, the femoral artery catheter was flushed with small volumes (100 µl) of heparinized saline (20 U/ml) in order to maintain recording fidelity.

After a 2-hour stabilization period, hemodynamic parameters, viz: MAP, CO, and HR, were measured at -30, -15, -1 min as baseline before dosing. L-NA dissolved in normal saline was infused through the femoral vein cannula at 2.5 (n = 3), 5 (n = 3), 10 (n = 4), and 20 mg/kg/hr (n = 4) in four groups of rats over a one-hour infusion interval. In all animals, the total volume of saline administered was held constant (3 ml) by varying the drug concentration in the infusion medium to achieve the desired L-NA dose. Control rats received 3 ml of normal saline over a one-hour infusion interval. Arterial blood samples (350 µl) were collected from the femoral artery catheter into heparinized syringes before dosing and at the following time points: 10, 20, 40, 60, 65, 80, 120, and 150 min in both control and L-NA treated animals. In each animal, the blood volume collected at each sampling time point was replaced by an equal volume of blood from a donor rat and hematocrit was measured after each sampling. Blood samples were centrifuged immediately (2 min, 13,000 g) and the plasma was stored at -20°C until analysis.

Pharmacokinetic (PK)-Pharmacodynamic (PD) Modeling

To describe the relationships between the plasma concentrations of L-NA and the hemodynamic effects, a nonparametric approach as described by Verotta and Sheiner (9) was used. Accordingly, the PK model was approximated nonparametrically by line segments joining the observed plasma concentrations at different time points (10). To account for the temporal delay (hysteresis) between plasma concentration and the measured hemodynamic effects, a hypothetical effect compartment was assumed to be linked to the plasma compartment by a first-order process as described by Sheiner et al. (11). The first-order rate constant, k_{eo} , was estimated nonparametrically as the value that best collapsed the hysteresis loop (11). The sigmoid E_{max} model was used to describe the relationships between

the concentrations at the hypothetical effect compartment (C_e) obtained after collapsing the hysteresis loop and the observed hemodynamic responses. Thus,

$$E = (E_{max} \cdot C_e^n) / (EC_{50}^n + C_e^n) \quad (1)$$

where E is the observed effect, E_{max} is the maximal effect, EC_{50} is the concentration causing half the maximal effect and n is the power function that determines the shape of the curve. The relationship between C_e and systemic vascular resistance SVR was described by the linear effect model:

$$E = E_0 + s C_e \quad (2)$$

where s represents the slope of the linear pharmacodynamic model and E_0 is the baseline effect value.

Data Analysis

Cardiac index (CI) was calculated from (CO/body weight in gm) \times 100. SVR was calculated from MAP/CI. The ADAPT computer program (Biomedical Simulations Resource, CA, U.S.A) was used to treat the experimental data.

RESULTS

Following a one-hour i.v. infusion of L-NA at 2.5, 5, 10, 20 mg/kg/hr in male rats, plasma concentrations of the drug slowly increased and maximum concentrations were achieved at the end of the infusion ($t = 60$ min; Fig. 1). Hemodynamic parameters, i.e. MAP, CI, and HR, measured in control animals receiving saline ($n = 3$) indicated that the baseline values of all the selected hemodynamic parameters remained stable over the study period (data not shown). Changes in MAP, CI, and HR after administration of L-NA are shown in Figure 2. After starting the L-NA infusion, MAP increased slowly in a dose-dependent manner until the maximum effect was reached at approximately 50 to 60 min after the start of infusion and remained steady until the end of the study (Fig. 2A). At the same time, there was a progressive and dose-dependent decrease in cardiac index which lasted until the end of study (Fig. 2B). Administration of L-NA at 20 mg/kg, the maximum dose,

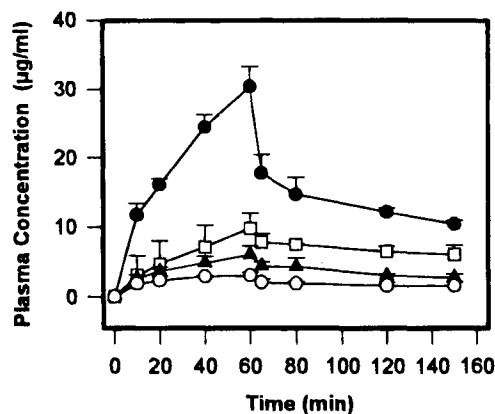


Fig. 1. Plasma concentration-time profile of L-NA in anesthetized rats after i.v. infusion of drug at four different doses. L-NA was infused at 2.5 (○, n = 3), 5 (▲, n = 3), 10 (□, n = 4), and 20 (●, n = 4) mg/kg/hr over a one-hour infusion interval in four groups of rats. Data are expressed as mean \pm S.D.

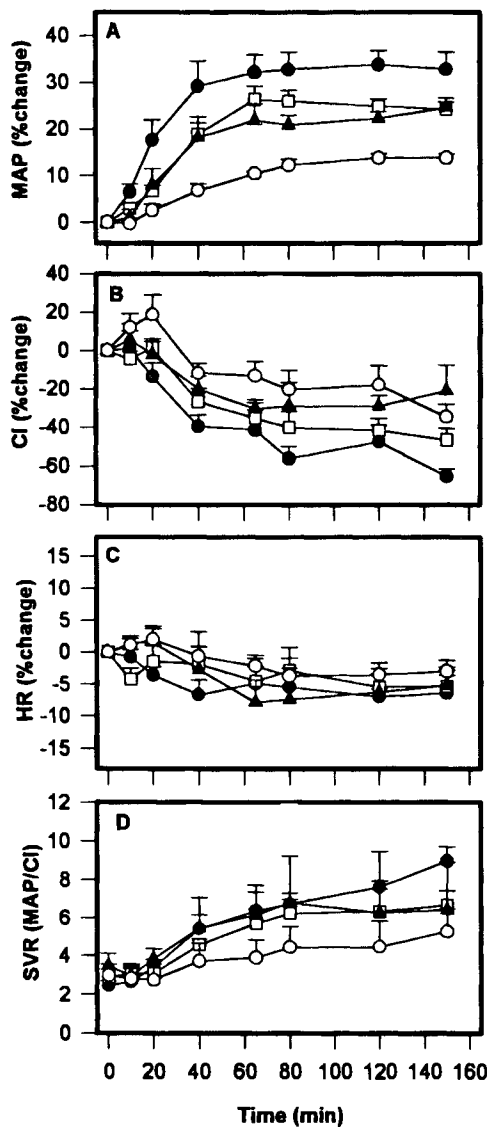


Fig. 2. Changes in the hemodynamic parameters after infusion of L-NA in anesthetized rats at four different doses: 2.5 (○, n = 3), 5 (▲, n = 3), 10 (□, n = 4), and 20 (●, n = 4) mg/kg/hr over a one-hour infusion interval. Key: (A) MAP = mean arterial pressure; (B) CI = cardiac index; (C) HR = heart rate, (D) SVR = systemic vascular resistance. Data are expressed as mean ± s.e.m.

resulted in a 30–40% increase in MAP and a 50–60% decrease in CI. Among all the hemodynamic parameters measured, HR was the least affected by L-NA infusion at all doses (Fig. 2C). SVR increased steadily in a dose-dependent manner and, at the higher doses, reached three to four times the baseline value (Fig. 2D).

The relationships between the hemodynamic effects measured and plasma L-NA concentration were not monotonic. Hysteresis was observed between the L-NA plasma concentration and all the hemodynamic parameters measured. A representative concentration-effect profile for MAP after administration of 20 mg/kg of L-NA is shown in Figure 3. Using a non-parametric PK/PD modeling approach, the hysteresis loop could be collapsed (Fig. 4). The equilibration half-time ($t_{1/2,keo}$) between plasma L-NA and the hypothetical effect site,

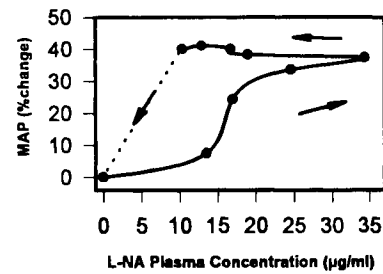


Fig. 3. A representative plot of the hysteresis loop observed in the relationship between L-NA plasma concentrations and MAP in one rat at 20 mg/kg.

according to this analysis, was 51.5 ± 6.6 min, 42.4 ± 10.1 min, 43.4 ± 9.0 min for MAP, CI, and SVR, respectively (n = 14).

After collapsing the hysteresis loop, the relationships between concentrations of L-NA at the hypothetical effect com-

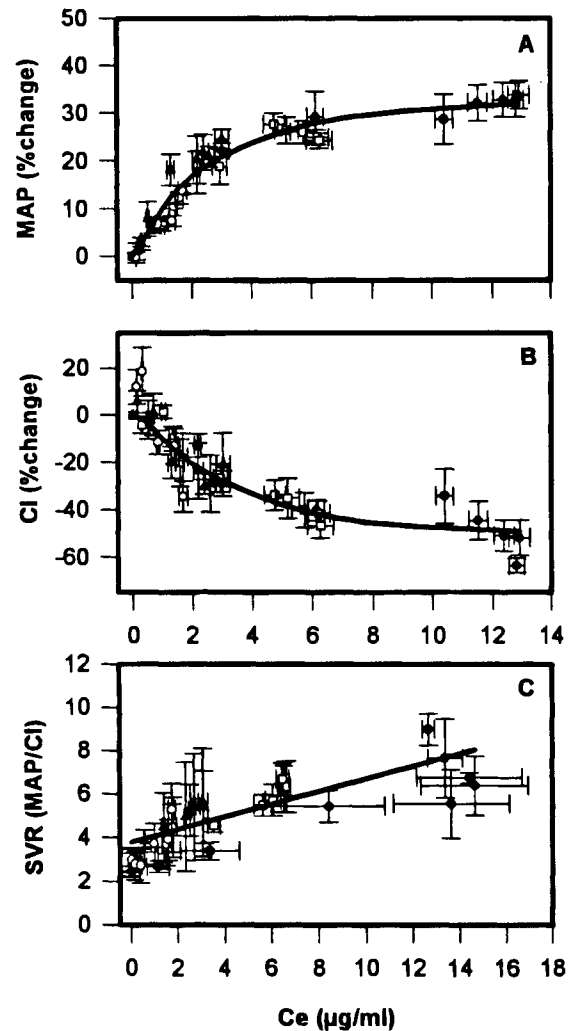


Fig. 4. Relationship between MAP (A), CI (B), or SVR (C) and the concentrations of L-NA at the hypothetical effect compartment described by the sigmoid E_{max} model (panel A or panel B) and the linear model (panel C). Solid lines represent the best fit of the model to the actual data when all the data were analyzed simultaneously (n = 14). Data are expressed as mean ± s.e.m.

partment (Ce) and MAP as well as CI can be best described by a sigmoid E_{max} model. Table I summarizes the parameter estimates obtained from nonlinear curve fitting of the relationship between MAP or CI effect data and Ce using the sigmoid E_{max} model. The E_{max} and EC_{50} values obtained were $+32.5 \pm 8.4\%$ and $2.6 \pm 1.3 \mu\text{g/ml}$ for MAP and $-52.9 \pm 15.6\%$ and $3.7 \pm 1.8 \mu\text{g/ml}$ for CI, respectively. Figure 4 shows the computer-fitted curves resulting from simultaneous analyses of all data for MAP (panel 4A) and CI (panel 4B) using the sigmoid E_{max} model. The relationship between SVR and Ce can be adequately described by a linear effect model (Fig. 4C); the slope and intercept obtained from simultaneous analyses of all the data were 0.29, and 3.8, respectively.

Figure 5A shows the relationship between the observed changes in MAP vs. CI over the study interval in all experiments. It is evident that the % changes in MAP and CI appeared to be linearly related to each other ($r = -0.932$). The slope of the regression line was -0.52 , indicating that the % changes in MAP (y-axis) were about half the magnitude of the changes in CI (the x-axis) in the study. Figure 5B shows the association between the observed changes in CI and SVR. Here, the relationship appeared non-linear; SVR continued to increase even when decreases in CI have gradually plateaued.

DISCUSSION

The use of NOS inhibitors in the treatment of septic shock has been controversial. While the induction of NOS and excessive production of NO have been implicated as causes of the severe hypotension that accompanied septic shock, inhibition of NOS is not always beneficial. For example, in a murine model of endotoxemia, i.v. bolus injection of a dose of 10 mg/kg of the methyl ester prodrug of L-NA resulted in a significant decrease in survival rate of the animals after endotoxin challenge (6). The proper dose range or plasma concentration that should be employed to avoid extensive tissue hypo-perfusion as a result of NOS inhibition has not been examined.

In this first pharmacokinetic/pharmacodynamic study involving a NOS inhibitor, we demonstrated that the relationships between L-NA plasma concentrations and the measured hemodynamic effects were complex and time-dependent. Consistent with the previous observations in rats, dogs and humans (4,12,13), L-NA administration in anesthetized rats produced substantial increases in MAP and SVR, pronounced decreases in CI, and minimal changes in the HR. An important finding

Table I. Pharmacodynamic Parameter Estimates Obtained from Non-linear Curve-Fitting of the Relationship Between MAP or CI Effect Data and the Concentration at the Hypothetical Effect Compartment (Ce) Using a Sigmoid E_{max} Model

Parameter	MAP \pm S. D. ^b	CI \pm S. D. ^b
E_{max} (% change)	$+32.5 \pm 8.4^a$	-52.9 ± 15.6^a
EC_{50} ($\mu\text{g/ml}$)	2.6 ± 1.3	3.7 ± 1.8
n	3.9 ± 3.9	3.5 ± 3.6

^a Denotes statistical significance (Student's t test, $p < 0.05$).

^b Pharmacodynamic parameters were obtained after analysis of the data from the individual animals receiving 20 and 10 mg/kg/hr dose (data are expressed as mean \pm S.D., $n = 8$).

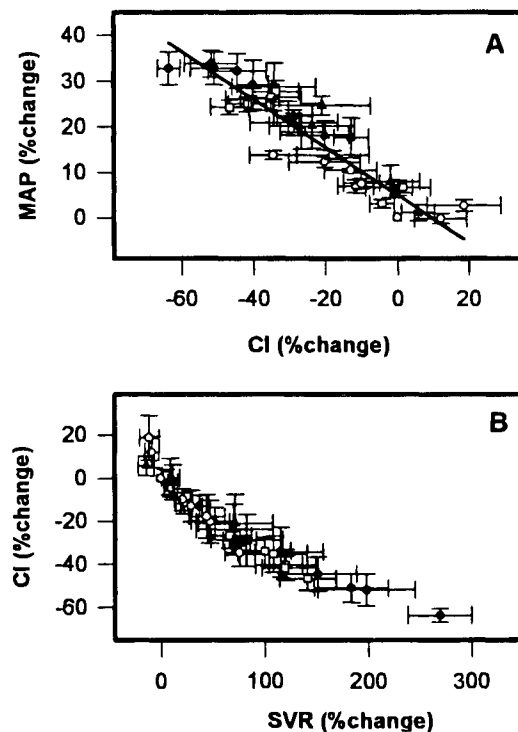


Fig. 5. Relationship between MAP and CI (A), and CI and SVR (B) in rats infused with L-NA ($n = 14$). The line in panel A is obtained from linear regression of MAP vs. CI. Data are expressed as mean \pm s.e.m.

in this study is that increases in MAP (the beneficial effect) were linearly related to decreases in CI (the unwanted side-effect), with a MAP/CI slope of approximately -0.52 . This result indicated that, at least in this animal model, gains in MAP effect could not be accomplished without accompanying decreases in CI over any concentration range of L-NA. This pharmacodynamic complication has led to the poor efficacy of NOS inhibitors when used as single agents for the treatment of septic shock (5–7).

The hysteresis loop observed between plasma L-NA concentration and hemodynamic effects was initially minimized through a nonparametric approach, which has the advantage that the concentration-effect relationship can be derived without any knowledge of the underlying pharmacokinetic or pharmacodynamic models. The relationship between the hypothetical effect concentration and the effect can then be inspected directly before selecting a particular pharmacodynamic model. Based on the sigmoidal shape of the derived hypothetical effect site concentration and MAP or CI effect relationships, a sigmoid E_{max} model was selected to quantify these relationships.

Temporal delays between measured plasma concentrations and effects may occur due to distribution of drug to and from the effect site (biophase), formation of active metabolite(s), receptor sensitization (14), or indirect pharmacological responses when the pharmacological effect requires time for development (15). Results obtained from *in vitro* investigations suggested that L-NA was neither chemically modified by NOS (16,17) nor was metabolized in tissue homogenates (unpublished data). Thus, formation of an active metabolite(s) of L-

NA is unlikely. For many drugs, the delay observed in the pharmacological responses is due to indirect mechanisms relating to the inhibition or stimulation of the production or dissipation of factors controlling the measured effects (18). The rapidly reversible actions induced by the biochemical intermediates involved in the NO-related responses, i.e. NO and cyclic guanosine monophosphate, cGMP (19), suggested that the indirect response pharmacodynamic models (18) may be less applicable for describing the effects measured after *in vivo* administration of L-NA. In the present study, the effect compartment model was employed to describe our experimental data; the basic assumption of this modeling approach as described by Sheiner et al. (11) is that the temporal delay observed between plasma concentration and effect is mainly due to the distribution of drug to and from the biophase via a first-order process. The transport of L-NA has been suggested to be mediated through the neutral amino-acid cellular transporter L system. It is therefore feasible that L-NA distribution into the site of action may represent a rate-determining step in its pharmacodynamics.

Our results showed that L-NA infusion increased SVR substantially and dose-dependently. Since SVR measures changes in MAP after normalization for changes in CI, this parameter can provide some mechanistic insights regarding the vascular vs. cardiac effects elicited by the NOS inhibitor. The increase in SVR observed in the present study was likely caused by the direct inhibition of NO generation at the vascular level since local administration of NOS inhibitors was previously shown to increase forearm vascular resistance in humans (20). Since it has been shown recently that *in vitro* NOS inhibition has little effect on the contractility of cardiac myocytes (21), the pronounced decrease in CI observed here may be secondary to the increase in afterload as a result of the intense increase in peripheral vascular resistance and not from the direct effect of the inhibitor on the heart itself (22).

Selection of an anesthetic agent in studies involving cardiovascular function is an important consideration since anesthetics can elicit changes in hemodynamic profiles. Single i.p. injection of thiobutobarbital was reported to induce a prolonged anesthetic effect and result in a stable physiological preparation when used in rats (23). In agreement with these results, hemodynamic parameters measured in control animals indicated that the animal preparation was stable and no detectable change was observed in the cardiovascular parameters measured throughout the study. A limitation of the present study was the short time interval of the study in comparison to the long elimination half-life of L-NA that we have reported previously (24,25). Unfortunately, longer duration of the study was not possible due to the lack of stability of the animal preparation employed here.

In summary, we have provided the first characterization of the pharmacokinetic/pharmacodynamic relationship of a NOS inhibitor, L-NA, in regard to its *in vivo* hemodynamic effects. Our results suggest that dose escalation of L-NA may be counter-productive since the depressant effect on CI may outweigh any therapeutic gains in MAP elevation. Further investigations are required to establish the concentration-effect relationships for L-NA and other NOS inhibitors in septic animals and humans. Such studies are crucial if NOS inhibitors are to be used optimally and effectively in the treatment of the deadly disease of septic shock.

ACKNOWLEDGMENTS

This work was supported in part by grant HL22273 from the National Institutes of Health. The authors acknowledge Dr. William F. Ebling for helpful discussions and Mr. David Soda for excellent assistance in animal surgery.

REFERENCES

1. S. Moncada and E. A. Higgs. Molecular mechanisms and therapeutic strategies related to nitric oxide. *FASEB J.* **9**:1319-30 (1995).
2. A. Petros, G. Lamb, A. Leone, S. Moncada, D. Bennett, and P. Vallance. Effects of a nitric oxide synthase inhibitor in humans with septic shock. *Cardiovas. Res.* **28**:34-9 (1994).
3. J. A. Lorente, L. Landin, R. De Pablo, E. Renes, and D. Liste. L-arginine pathway in the sepsis syndrome. *Crit. Care Med.* **21**:1287-95 (1993).
4. R. E. Klabunde, R. C. Ritger, and M. C. Helgren. Cardiovascular actions of inhibitors of endothelium-derived relaxing factor (nitric oxide) formation/release in anesthetized dogs. *Eur. J. Pharmacol.* **199**:51-9 (1991).
5. R. G. Kilbourn, C. Szabo, and D. L. Traber. Beneficial versus detrimental effects of nitric oxide synthase inhibitors in circulatory shock: lessons learned from experimental and clinical studies. *Shock* **7**:235-46 (1997).
6. E. A. Minnard, J. Shou, H. Naama, A. Cech, H. Gallagher, and J. M. Daly. Inhibition of nitric oxide synthesis is detrimental during endotoxemia. *Arch. Surg.* **129**:142-7 (1994).
7. F. M. Robertson, P. J. Offner, D. P. Ciceri, W. K. Becker, and B. A. Pruitt, Jr. Detrimental hemodynamic effects of nitric oxide synthase inhibition in septic shock. *Arch. Surg.* **129**:149-55 (1994).
8. M. A. Tabrizi-Fard and H. L. Fung. Reversed-phase high-performance liquid chromatography method for the analysis of nitro-arginine in rat plasma and urine. *J. Chromatog. B: Biom. Applic.* **679**:7-12 (1996).
9. D. Verotta and L. B. Sheiner. Simultaneous modeling of pharmacokinetics and pharmacodynamics: an improved algorithm. *CABIOS* **3**:345-9 (1987).
10. J. D. Unadkat, F. Bartha, and L. B. Sheiner. Simultaneous modeling of pharmacokinetics and pharmacodynamics with nonparametric kinetic and dynamic models. *Clin. Pharmacol. Ther.* **40**:86-93 (1986).
11. L. B. Sheiner, D. R. Stanski, S. Vozeh, R. D. Miller, and J. Ham. Simultaneous modeling of pharmacokinetics and pharmacodynamics: application to d-tubocurarine. *Clin. Pharmacol. Ther.* **25**:358-71 (1979).
12. W. G. Haynes, J. P. Noon, B. R. Walker, and D. J. Webb. Inhibition of nitric oxide synthesis increases blood pressure in healthy humans. *J. Hypertension.* **11**:1375-80 (1993).
13. H. M. Vargas, J. M. Cuevas, L. J. Ignarro, and G. Chaudhuri. Comparison of the inhibitory potencies of N(G)-methyl-, N(G)-nitro- and N(G)-amino-L-arginine on EDRF function in the rat: evidence for continuous basal EDRF release. *Journal of Pharmacology & Experimental Therapeutics.* **257**:1208-15 (1991).
14. N. H. Holford and L. B. Sheiner. Understanding the dose-effect relationship: clinical application of pharmacokinetic-pharmacodynamic models. *Clin. Pharmacokin.* **6**:429-53 (1981).
15. W. J. Jusko and H. C. Ko. Physiologic indirect response models characterize diverse types of pharmacodynamic effects. *Clin. Pharmacol. Ther.* **56**:406-19 (1994).
16. P. Klatt, K. Schmidt, F. Brunner, and B. Mayer. Inhibitors of brain nitric oxide synthase. Binding kinetics, metabolism, and enzyme inactivation. *J. Biol. Chem.* **269**:1674-80 (1994).
17. E. S. Furfine, M. F. Harmon, J. E. Paith, and E. P. Garvey. Selective inhibition of constitutive nitric oxide synthase by L-NG-nitroarginine. *Biochemistry.* **32**:8512-7 (1993).
18. N. L. Dayneka, V. Garg, and W. J. Jusko. Comparison of four basic models of indirect pharmacodynamic responses. *J. Pharmacokin. Biopharm.* **21**:457-78 (1993).

19. T. B. Tzeng and H. L. Fung. Pharmacodynamic modeling of the in vitro vasodilating effects of organic mononitrates. *J. Pharmacokin. Biopharm.* **20**:227-51 (1992).
20. P. Vallance, J. Collier, and S. Moncada. Effects of endothelium-derived nitric oxide on peripheral arteriolar tone in man. *Lancet.* **2**:997-1000 (1989).
21. A. J. Brady, P. A. Poole-Wilson, S. E. Harding, and J. B. Warren. Nitric oxide production within cardiac myocytes reduces their contractility in endotoxemia. *Am. J. Physiol.* **263**:H1963-6 (1992).
22. S. M. Gardiner, A. M. Compton, P. A. Kemp, and T. Bennett. Regional and cardiac haemodynamic effects of NG-nitro-L-arginine methyl ester in conscious, Long Evans rats. *Brit. J. Pharmacol.* **101**:625-31 (1990).
23. J. Buelke-Sam, J. F. Holson, J. J. Bazare, and J. F. Young. Comparative stability of physiological parameters during sustained anesthesia in rats. *Lab. Anim. Sci.* **28**:157-62 (1978).
24. M. A. Tabrizi-Fard and H. L. Fung. Pharmacokinetics, plasma protein binding and urinary excretion of N omega-nitro-L-arginine in rats. *Brit. J. Pharmacol.* **111**:394-6 (1994).
25. M. A. Tabrizi-Fard and H. L. Fung. Pharmacokinetics and steady-state tissue distribution of L- and D-isomers of nitroarginine in rats. *Drug Metab. Dispos.* **24**:1241-6 (1996).